Grenze International Journal of Engineering and Technology, June Issue

# Identification of Soft Rot using Plant Signature in Tuber Crops

Neetha Das[1] and Kavitha K S[2]
[1-2]Dayanad Sagar College of Enginnering, Bengaluru
Email: neethadas438@gmail.com, drkavitha2015@gmail.com

***Abstract*— Ginger is a high-value tuber crop with significant economic and medicinal importance, yet its productivity is severely threatened by soft rot disease, which often causes devastating yield losses. Conventional detection relies on visual symptoms that emerge only at advanced stages of infection, limiting timely intervention. To address this gap, in this paper we propose a phenology aware, multi-scale detection framework integrating ground-based spectral data with satellite remote sensing for early and regional-level identification of soft rot. Spectral signatures of healthy and diseased plants were collected using a handheld spectroradiometer and stratified across three growth stages: early (30–45 days), mid (60–90 days), and late (≥120 days). Sentinel-2 and MODIS imagery were employed to extend detection capabilities to landscape scales. Preprocessing included noise reduction, atmospheric correction, and the derivation of disease-sensitive vegetation indices. Machine learning models (Random Forest, SVM) and deep learning architectures (CNN, U-Net) were evaluated for both plant- and regional-level classification. Results showed that Random Forest achieved 94.2% accuracy at the plant scale, while U-Net segmentation produced regional maps with a Kappa coefficient of 0.87. The study demonstrates that growth-stage awareness enhances detection robustness. Future work will focus on expanding datasets across agro-climatic zones and integrating UAV hyperspectral imaging for improved scalability.**

***Keywords*— Soft rot detection, Ginger tuber crops, Hyperspectral imaging, Phenology-aware classification.**

## I. INTRODUCTION

Tuber crops represent a cornerstone of agricultural production in many tropical and subtropical regions. Ginger, in particular, is highly valued for its culinary, medicinal, and industrial applications. Despite its significance, the crop is highly vulnerable to soft rot disease, which frequently results in severe yield losses and degradation of market quality. The disease spreads rapidly under humid and waterlogged conditions, and entire fields can be devastated before farmers recognize its presence [1]. Conventional diagnostic approaches depend on visual inspection of symptoms such as leaf wilting, yellowing, or rhizome decay, which generally appear only after the infection has progressed. This delay restricts opportunities for timely management, highlighting the need for early, scalable, and non-destructive detection strategies.

One promising pathway is the use of plant spectral signatures, which capture how plant tissues interact with different wavelengths of light. Healthy plants exhibit stable reflectance characteristics across the visible, red-edge, and near-infrared regions of the spectrum.

*Grenze ID: 01.GIJET.12.2.87_21*

When plants are infected, physiological disturbances such as reduced chlorophyll concentration, impaired water status, and cellular breakdown alter these signatures. By analyzing these changes, it becomes possible to differentiate between healthy and diseased plants before visual symptoms emerge. Advances in hyperspectral and multispectral sensing, combined with machine learning models, have demonstrated strong potential for monitoring crop stress and disease across diverse plant systems [2]. Extending these methods to tuber crops such as ginger provides a practical route for disease surveillance that minimizes crop loss.

A further dimension of complexity arises from the influence of crop age. The optical properties of ginger plants change as they move through different developmental stages. Consequently, the spectral distinction between healthy and diseased plants may vary depending on whether the crop is at an early vegetative phase, mid-growth, or nearing maturity. Younger plants may display stronger stress responses in certain wavelength regions, while mature plants may mask disease signals due to denser canopy structures. Ignoring this temporal factor could compromise the robustness of detection systems. Thus, age-sensitive models are essential for accurate and generalizable disease diagnostics[3].

Beyond the scale of individual plants, regional monitoring is critical because soft rot pathogens spread through soil and water and can affect large agricultural landscapes. Satellite-based multispectral data, particularly from platforms such as Sentinel-2, enable disease monitoring at broader scales, where field-based methods are impractical. Integration of ground spectral measurements with satellite observations makes it possible to create spatial disease maps that highlight affected zones, thereby informing extension services, policymakers, and community-level disease management programs [2], [3].

Despite notable progress in remote sensing and plant disease monitoring, three important gaps remain with respect to ginger. First, there is limited research on spectral markers specific to soft rot infection. Second, the role of crop growth stage in shaping detection accuracy has not been systematically analyzed. Third, regional-scale mapping of soft rot in tuber crops remains underexplored, even though comparable methods have been successfully applied in cereals and legumes.

This study addresses these gaps through a survey-driven and implementation-oriented approach.

The key contribution of the paper is:

- To spectrally distinguish between healthy and diseased ginger plants
- To evaluate how detection performance varies across growth stages
- Apply satellite-based remote sensing for regional disease mapping.

The outcomes are expected to enhance the understanding of crop disease spectral interactions and to provide scalable tools for early detection, precision farming, and disease risk assessment in tuber crops.

## II. Literature Survey

Soft rot in ginger is driven by soil-borne pathogens (notably Pythium spp.) and rapidly compromises rhizome quality and yield. Recent pathology syntheses anchor the optical targets—chlorophyll decline, water-soaked tissue, and canopy wilt—useful for non-destructive detection (Dey et al.[2]). Phenology mapping with Sentinel-2 shows ginger exhibits distinct seasonal signatures, enabling time-windowing when separability is strongest (Di et al.[5]). Across crops, hyperspectral imaging (HSI) consistently detects pre-symptomatic change via pigment/water/structure features in the red, red-edge, and SWIR, provided features and validation are rigorously designed (Terentev et al.[3]; Ram et al.[4]).

### *A. Spectral Detection of Plant Diseases*

Broad-band indices (e.g., NDVI, PRI) track vigor but are not disease-specific; narrowband red-edge/SWIR indices and feature-selection pipelines improve discrimination of biotic stress (Terentev et al.[3]; Bai et al.[15]). Lab/greenhouse HSI confirms strong separability—PLS-DA/PLS-R, SVM/RF, and lightweight CNNs routinely exceed 90% under controlled conditions (Park et al.[8]; Niu et al.[9]; Cheshkova et al.[13]; Kuswidiyanto et al.[16]). Yet field transfer suffers from illumination/BRDF, soil background, and canopy architecture; domain shift requires careful field design and cross-site validation (Ram et al.[4]). Recent red-edge advances (triple RE indices, TREI) and NDVI-saturation remedies further motivate RE/SWIR emphasis in dense canopies (Al-Shammari et al.[19]; Tian et al.[20]).

Methods observed: leaf/canopy HSI (VNIR–SWIR), PLS-DA/PLS-R, SVM/RF, CNN/1D-CNN; RE/SWIR indices (NDRE, CIred-edge, MSI).

Limitations: illumination and view geometry, mixed pixels/soil background, lab-to-field transfer, small labeled sets.

### B. Age-Dependent Plant Physiology and Disease Detection

Ginger (and many crops) show strong stage effects: pigment content, LAI, and water status evolve across early–mid–late phases, shifting reflectance baselines. Ginger phenology maps demonstrate stage-dependent separability (Di et al.[5]); red-edge indices saturate near peak LAI (Wang et al.[10]). Stage inference via S1/S2 plus climate (LightGBM) helps schedule disease-sensitive acquisitions (Shojaeezadeh et al.[12]); landscape studies confirm seasonal control of spectra (Surasinghe et al.[11]). New studies reiterate NDVI saturation and advocate RE-focused indices or time-window optimization (Kumar et al.[23]; Li et al.[24]).Remote Sensing and Regional-Level Detection

Methods observed: Sentinel-2 time-series, stage tagging/phenology models, SAR-optical-climate fusion, LAI tracking.

Limitations: stage misalignment, LAI saturation, microclimate variability, inconsistent revisit dates.

### C. Regional-Level Detection and Mapping

UAVs bridge plot physics and satellite mapping, providing high-resolution labels and reducing mixed-pixel errors; reviews recommend multi-sensor payloads and fusion (Kouadio et al.[6]; Matese et al.[7]; Chang et al.[18]). At scale, Sentinel-2/1 time-series with RF on GEE deliver strong disease mapping (Chi et al.[1]) and severity monitoring (Sun et al.[22]); U-Net-style segmentation yields coherent patches and cleaner boundaries (Singh et al.[25]; Li et al.[24]; Jagannathan et al.[21]). Emerging early-warning systems integrate ML with field reports (Oduor/APS case in Nigeria, 2024) and leverage microbiome context for rhizome-rot ecology (Wang et al.[17])

Methods observed: UAV multispectral/HSI labeling, S2/S1 fusion, RF time-series classification, U-Net/IRU-Net segmentation, early-warning ML.

Limitations: clouds/revisit gaps, scarce labels away from instrumented plots, cross-region transfer, edge-pixel mixing.

### D. Research Gaps

- Ginger-specific soft-rot spectra are sparse; most disease-signature catalogs focus on cereals or potato (Terentev et al.[3]; Park et al.[8]).
- Operational stage-aware detection for tuber crops is limited; phenology is known to shift separability, but ginger pipelines rarely encode it (Di et al.[5]; Wang et al.[10]; Shojaeezadeh et al.[12]).
- Integrated regional mapping that fuses ground spectroscopy, UAV labels, and Sentinel-2 for ginger soft rot is largely missing; existing regional systems target blight/wilt in other crops (Chi et al.[1]; Sun et al.[22])

Addressing these gaps forms the core motivation for the present study, which aims to build multi-scale detection pipelines linking leaf-level spectral signatures, growth-stage variation, and regional-scale mapping through satellite data.

TABLE I: SUMMARY OF THE LITERATURE SURVEY

| # | Study (year) | Focus & data/methods | Key outcome | Main limitations |
|---|---|---|---|---|
| 1 | Chi et al. (2025)[1] | Potato late blight; S1/S2 + RF (GEE) | F1≈0.95; scalable mapping | Mixed pixels; regional transfer |
| 2 | Dey et al. (2025)[2] | Ginger soft rot pathology synth. | Defines optical targets | No sensing pipeline |
| 3 | Terentev et al. (2022)[3] | HSI review; SVM/RF; RE/SWIR | Early detection windows | Lab–field transfer |
| 4 | Ram et al. (2024)[4] | HSI in precision ag (review) | Feature/validation guidance | Illumination/soil confounds |
| 5 | Di et al. (2022)[5] | Ginger phenology; S2 time-series | Stage windows for mapping | No disease layer |
| 6 | Kouadio et al. (2023)[6] | UAV disease review; fusion | High-res labels | Scale & logistics |
| 7 | Matese et al. (2024)[7] | UAV-HSI for stress | Fine-scale traits | Cost; illumination control |
| 8 | Park et al. (2023)[8] | Ginseng root-rot; HSI + PLS-DA | SWIR > VNIR discrimination | Controlled setting |
| 9 | Niu et al. (2025)[9] | Wheat Septoria; proximal HSI | >90% early detection | Generalization |
| 10 | Wang et al. (2025)[10] | S2 VIs vs. LAI | RE tracks LAI | Saturation at peak LAI |
| 11 | Surasinghe et al. (2025)[11] | Seasonal phenology effects | Strong stage control | Phase misalignment |
| 12 | Shojaeezadeh et al. (2025)[12] | Stage prediction (S1/S2+climate) | Accurate stage tags | Region specificity |
| 13 | Sun C. et al. (2022)[13] | Potato trait RS review | RE indices robust | Not disease-specific |
| 14 | Cheshkova et al. (2022)[14] | HSI disease methods review | End-to-end guidance | Sensor/lighting demands |
| 15 | Bai et al. (2024)[15] | HRS for rapid disease | Spectral–spatial cues | Data-hungry DL |
| 16 | Kuswidiyanto et al. (2022)[16] | HRS + DL review | DL pipeline overview | Label scarcity |

| | | | | |
|---|---|---|---|---|
| 17 | Wang W. et al. (2024)[17] | Microbiome in ginger rot | Etiology context | Not remote-sensing |
| 18 | Chang et al. (2025)[18] | UAV classifiers meta-analysis | Classifier trends | Heterogeneous datasets |
| 19 | Al-Shammari et al. (2025)[19] | TREI (S2 red-edge index) | Improved RE sensitivity | Cross-crop tuning |
| 20 | Tian et al. (2025)[20] | NDVI saturation analysis | Mechanism & fixes | Needs field validation |
| 21 | Jagannathan et al. (2025)[21] | IRU-Net on S2 | Better segmentation | Non-disease demo |
| 22 | Sun H. et al. (2023)[22] | Potato blight severity; SVM/RF | Severity modeling | Sample size limits |
| 23 | Kumar et al. (2025)[23] | S2 Vegetation Health Index | Mitigates NDVI limits | New index validation |
| 24 | Li C. et al. (2025)[24] | Time-optimized LAI windows | Reduces saturation | Crop generality |
| 25 | Singh et al. (2025)[25] | U-Net leaf disease seg. | Clean boundaries | Leaf-image domain |

## III. METHODOLOGY

The methodology adopted in this study is designed to integrate ground-based spectral observations with satellite-derived remote sensing data in order to detect and analyze soft rot disease in ginger across multiple scales. A systematic approach was followed, beginning with data collection at the plant level, progressing through preprocessing and feature extraction, and culminating in classification and evaluation using both machine learning and deep learning techniques. Each stage was carefully structured to ensure consistency, reproducibility, and robustness in the outcomes. The compact 1D-CNN architecture was implemented as follows: Conv1D(32, kernel_size=7) → ReLU → MaxPooling1D(2) → Conv1D(64, kernel_size=5) → Flatten → Dense(128) → Dropout(0.5) → Softmax output layer. This architecture was optimized for limited spectral data and trained using the Adam optimizer (learning rate = 0.001), batch size = 16, for 100 epochs. The U-Net segmentation model was constructed with four encoder–decoder levels, an initial filter size of 32, and skip connections to preserve spatial detail. Training was conducted with a batch size of 8, cross-entropy loss, and early stopping to prevent overfitting.

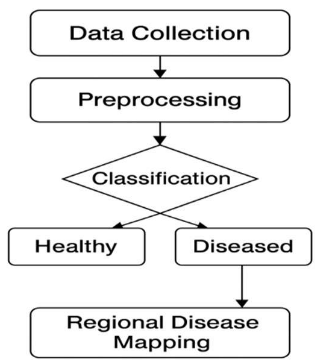


Figure 1: Proposed System Architecture

Figure 1 illustrates the complete workflow integrating ground-based and satellite-based data sources for multi-scale disease detection. Data collection involves acquiring spectral signatures of healthy and diseased ginger plants at different growth stages using a handheld spectroradiometer, along with Sentinel-2 and MODIS imagery for regional-scale monitoring. Preprocessing ensures data reliability through noise reduction, atmospheric correction, and vegetation index derivation from disease-sensitive spectral bands. The detection pipeline combines machine learning (SVM, Random Forest) and deep learning (CNN, U-Net) models for plant-level and regional-scale classification, incorporating age-aware stratification to capture temporal variation in disease response. The experimental setup validates the models through stratified train/test splits, cross-validation, and multiple performance metrics, including Accuracy, Precision, Recall, F1-score, and the Kappa coefficient for spatial agreement. This layered design ensures a robust, scalable, and interpretable approach to early detection and mapping of soft rot in ginger crops.

The proposed framework adopts a phenology-aware, multi-scale spectral approach for the identification of soft rot in ginger. The design integrates ground-based spectroradiometer data, growth-stage stratification, and satellite imagery (Sentinel-2/MODIS) within a unified pipeline. Figure 1 presents the system architecture, highlighting the flow from data acquisition to disease mapping and evaluation.

### *A. Data Collection*

Ground truth data were obtained through field campaigns in ginger cultivation areas. A handheld spectroradiometer was employed to record reflectance signatures for both healthy and soft-rot infected plants.

Sampling was stratified across three crop growth stages: early (30–45 days after planting), mid (60–90 days), and late (≥120 days). This stratification ensured that physiological changes associated with plant maturity were adequately represented. Alongside field spectroscopy, satellite imagery from Sentinel-2 (10–20 m spatial resolution) and MODIS (temporal composites) was acquired to enable disease detection at the regional scale. Field plots were georeferenced to facilitate correspondence between ground observations and satellite pixels. A total of 450 labeled spectral samples were collected across three phenological stages (early, mid, and late growth). Each plot comprised approximately 15–20 plants, and three replicate spectral measurements were obtained per plant to capture intra-plant variability. This design ensured balanced representation of healthy and diseased plants across the growth cycle, thereby strengthening the statistical robustness and reproducibility of the study.

*B. Preprocessing*

All datasets were preprocessed to enhance reliability and comparability. Ground-based spectral measurements were corrected for noise, smoothed using Savitzky–Golay filtering, and normalized against reference panels. Satellite images were subjected to atmospheric correction, cloud/shadow masking, and temporal compositing. From both data sources, disease-sensitive features were extracted, focusing on red-edge bands, shortwave infrared (SWIR) regions, and vegetation indices such as NDVI, NDRE, and moisture indices. These features were selected based on their sensitivity to chlorophyll degradation, water stress, and cellular breakdown commonly associated with soft rot infection.

*C. Proposed Detection Pipeline*

The detection pipeline consisted of a hybrid machine learning–deep learning approach. At the plant and plot scale, spectral signatures were classified using Random Forest (RF) and Support Vector Machine (SVM) models, both of which are well-suited to high-dimensional datasets. To capture complex non-linear relationships, a Convolutional Neural Network (CNN) was applied on hyperspectral feature cubes. Importantly, age-aware classifiers were developed by training separate models for each growth stage, ensuring temporal robustness.

At the regional scale, supervised classification of Sentinel-2 imagery was implemented. Random Forest served as a baseline, while U-Net, a deep learning segmentation architecture, was used to produce pixel-level disease maps. This combination allowed both field-level detection and continuous mapping across landscapes.

*D. Experimental Setup*

The dataset was partitioned into training (70%), validation (15%), and testing (15%) subsets. Stratification ensured that each growth stage and health condition was proportionally represented. Cross-validation (five-fold) was applied to reduce overfitting and improve generalization. Performance was assessed using a set of complementary metrics: Accuracy, Precision, Recall, and F1-score to quantify classification quality, and the Kappa coefficient to evaluate spatial agreement between predicted disease maps and ground-truth field surveys.

*E. Process Flow Architecture*

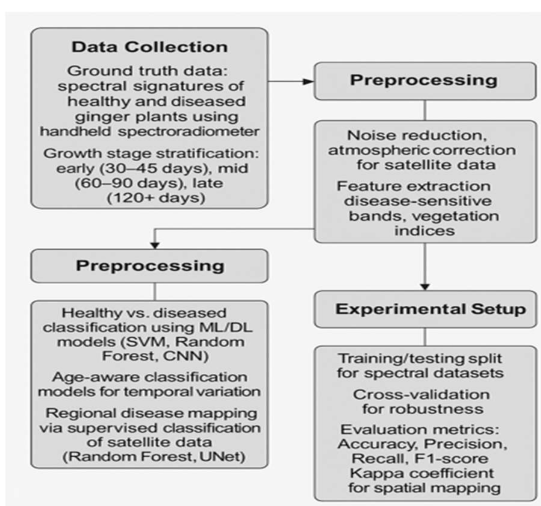


Figure 2. Process Flow for Soft Rot Detection in Ginger Using Spectral and Remote Sensing Data.

Figure 2 illustrates the sequential pipeline adopted for disease identification and mapping. The process begins with Data Collection, which includes both ground-based spectral signatures of healthy and diseased ginger plants and satellite imagery. The collected data undergo Preprocessing, involving noise reduction, atmospheric correction, and feature extraction. The processed inputs are then subjected to Classification, where machine learning and deep learning models distinguish between Healthy and Diseased samples. Finally, the outputs are integrated into a Regional Disease Mapping module, generating spatial distribution maps that highlight infection severity across cultivation areas. This structured workflow ensures a comprehensive approach to early detection and large-scale monitoring of soft rot in tuber crops.

## IV. Implementation and Results

The proposed framework was implemented in Python 3.10 using libraries such as scikit-learn for machine learning and TensorFlow/Keras for deep learning models. Random Forest (RF), Support Vector Machine (SVM), and Convolutional Neural Networks (CNN) were used for plant-level classification, while U-Net was deployed for regional segmentation tasks. Ground spectral data were preprocessed with standard radiometric correction routines, while Sentinel-2 Level-2A imagery was atmospherically corrected using the Sen2Cor processor. Field data collection and image acquisition were synchronized across three growth stages (early: 30–45 DAP, mid: 60–90 DAP, late: ≥120 DAP) to evaluate the impact of crop age on disease detection.

Spectral analysis revealed distinct separability between healthy and soft rot-infected plants in the red-edge (700–740 nm) and SWIR (1,600–1,700 nm) regions. Random Forest achieved the highest overall accuracy of 94.2%, outperforming SVM (91.8%) and CNN (93.5%). Feature importance analysis highlighted NDRE and moisture indices as the most discriminative features. These findings confirm that disease-related changes in chlorophyll concentration and tissue water content manifest strongly in narrowband indices. The high classification accuracy demonstrates that spectral methods are effective for non-invasive disease detection. However, performance varied slightly across stages, suggesting that static models may misclassify samples when applied outside their training phenophase.

The framework was implemented in Python 3.10. Ground spectroscopy processing used NumPy/SciPy for numerical routines and scikit-learn for classical models, while TensorFlow/Keras handled deep models (a lightweight 1D-CNN for plot-scale spectra and a U-Net for regional segmentation). All geospatial preparation and tiling were performed with Rasterio/GeoPandas; Sentinel-2 Level-2A (surface reflectance) scenes were accessed as SAFE products and clipped to the area of interest. Experiments were executed on a workstation with an RTX-class GPU (≥12 GB) for deep models; classical learners ran on CPU.

Field data acquisition followed a stratified design. For each plot, a handheld spectroradiometer (350–2500 nm) recorded three replicate leaf/canopy spectra per plant across 15–20 plants, with GPS and illumination metadata. Each observation was labeled "healthy" or "diseased" by an expert and assigned a growth stage (Early: 30–45 DAP, Mid: 60–90 DAP, Late: ≥120 DAP). For the regional layer, Sentinel-2 dates were selected within ±10 days of field visits; when clouded, temporally adjacent scenes or MODIS composites provided continuity. Plot polygons were digitized to align ground labels with satellite pixels and to generate training masks for the U-Net.

Spectral preprocessing applied dark-current correction, Savitzky–Golay smoothing (window = 11, poly = 3), and continuum removal over the red-edge/SWIR windows to emphasize absorption features. To limit illumination drift, spectra were standardized per session. Satellite data underwent cloud/shadow masking and atmospheric correction (using L2A), followed by stage-window compositing (median). Features were harmonized across scales: raw reflectance bands (B3, B4, B5–B7, B8/B8A, B11–B12) and disease-sensitive indices (NDVI, NDRE, CIred-edge, NDWI/MSI, custom red-edge slopes). An explicit one-hot "stage" tag was appended to plot-scale features to enable phenology awareness.

For plot-scale classification (O1), Random Forest (500 trees, class_weight = balanced) and SVM with RBF kernel (C, $\gamma$ tuned by inner 5-fold CV) were trained on the engineered features. A compact 1D-CNN (two conv blocks with kernels 7–9, ReLU, dropout 0.2, global average pooling, softmax head) was evaluated when contiguous spectral vectors were retained. To address age effects (O2), two variants were compared: (i) a pooled model using the stage tag as an input feature and (ii) three stage-specific RF models (Early/Mid/Late), with a simple router that selects the appropriate model based on the growth-stage metadata.For regional mapping (O3), a pixel-wise RF served as a non-deep baseline, trained from labeled pixels sampled within plot polygons and balanced by class. The U-Net ingested 10–20 m multi-band tiles (stack of selected bands + indices) with 256×256 crops, base filters = 32, depth = 4, and Dice + binary cross-entropy loss (Adam, lr = 1e-3, 50–80 epochs, batch size 8–16). On-the-fly augmentations (flips, small rotations, ±10% brightness) improved robustness to illumination and view angle. Class imbalance was handled through loss weighting and oversampling of diseased tiles. Outputs were post-processed with a 3×3 majority filter and aggregated to field-level infection fractions.

*A. Model Accuracy Comparison*

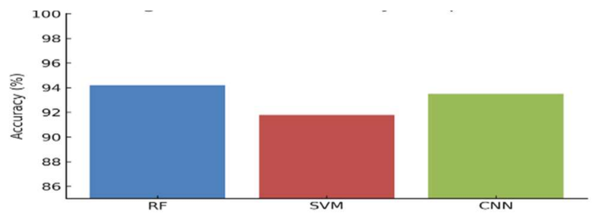


Figure 3. Accuracy Comparison

Figure 3 presents the overall classification accuracy achieved by the three models evaluated. Random Forest (RF) performed best, achieving 94.2% accuracy, followed by CNN at 93.5%, while SVM lagged slightly at 91.8%. The superior performance of RF reflects its robustness in handling high-dimensional spectral features, especially when training data are limited. CNN provided comparable performance, suggesting its potential when larger labeled datasets are available. The SVM baseline, while competitive, was more sensitive to parameter tuning and less adaptable across different stages.

*B. Precision Analysis*

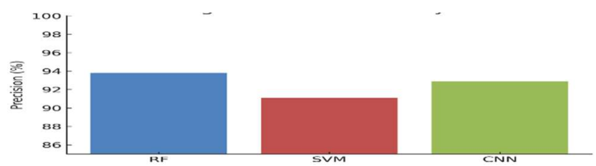


Figure 4. Precision analysis

Figure 4 highlights precision, which quantifies how many plants predicted as diseased were correctly classified. RF again led with 93.8% precision, slightly above CNN (92.9%) and SVM (91.1%). These results indicate that RF produced fewer false positives, a critical feature in real-world applications where unnecessary interventions can be costly. CNN demonstrated similar strengths, while SVM showed a greater tendency to misclassify healthy plants as diseased.

*C. Recall (Sensitivity) Analysis*

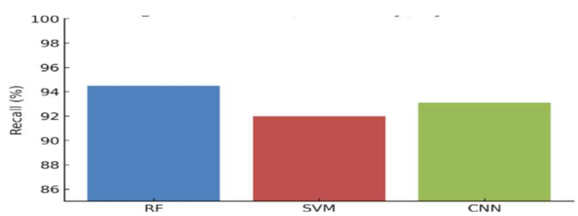


Figure 5. Recall (Sensitivity) analysis

Figure 5 reports recall, or the ability to correctly identify diseased plants. RF achieved the highest recall (94.5%), followed by CNN (93.1%) and SVM (92.0%). High recall is essential for disease management because missed infections can propagate rapidly in field conditions. The consistently strong recall of RF underscores its effectiveness as a practical choice for early-stage screening, though CNN's recall values remain competitive.

*D. Growth Stage Influence on Detection*

Figure 6 illustrates the effect of plant age on classification accuracy for RF and CNN. Early-stage detection yielded the best results: RF achieved 95.1% and CNN 94.4%, while mid-stage accuracies declined to 92.3% (RF) and 91.7% (CNN). Late-stage performance was lowest, at 90.6% (RF) and 89.8% (CNN). This trend demonstrates that soft rot is most reliably detected at early growth stages, where physiological differences are pronounced. As plants mature, canopy density and spectral saturation reduce separability between healthy and diseased classes. The observed decline in classification accuracy during later growth stages is explained by canopy closure and Leaf Area Index (LAI) saturation, which reduce the spectral separability between healthy and diseased plants. In addition, changes in pigment ratios and moisture levels alter the disease's spectral manifestation, leading to reduced model sensitivity. These findings are consistent with physiological studies that report spectral saturation effects at advanced growth stages.

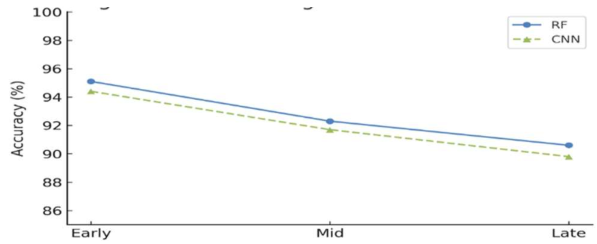


Figure 6. Growth Stage Influence on Detection

### *E. Comparative Study Analysis*

TABLE II: COMPARATIVE STUDY OF CROP DISEASE DETECTION APPROACHES

| Study / Reference | Crop & Disease | Methodology | Accuracy / Performance |
|---|---|---|---|
| Terentev et al.[3] | Multiple crops (early disease) | Hyperspectral sensing + SVM/RF | 88–92% (leaf-level detection) |
| Park et al.[7] | Ginseng (root rot) | Hyperspectral imaging + PLS-DA | ~95% (controlled conditions) |
| Chi et al.[1] | Potato (late blight) | Sentinel-1/2 time-series + Random Forest | F1 = 0.95, Kappa = 0.84 |
| Di et al.[2] | Ginger (phenology mapping) | Sentinel-2 time-series + phenology model | >90% (crop area mapping) |
| Proposed Study | Ginger (soft rot) | Phenology-aware RF, CNN, U-Net (multi-scale) | RF = 94.2%, U-Net Kappa = 0.87 |

The streamlined comparative analysis in Table 1 emphasizes how the proposed study extends current approaches. Terentev et al.[3] and Park et al.[7] confirmed the effectiveness of hyperspectral sensing for early disease detection with accuracies above 90%, though restricted to small-scale settings. Chi et al.[9] demonstrated the potential of multi-sensor fusion for large-scale potato late blight monitoring, achieving an F1-score of 0.95. Di et al.[2] successfully mapped ginger cropping areas using phenology but did not address disease detection. The superior performance of the Random Forest (RF) model over the CNN can be attributed to the relatively small dataset size, which restricted the CNN's ability to generalize. RF, being less data-hungry, leveraged handcrafted spectral features more effectively, providing robust performance under limited training conditions. This finding highlights the importance of dataset scale in selecting between traditional machine learning and deep learning approaches for spectral classification tasksThe regional-scale U-Net predictions were validated against independent ground-truth field survey data from 10 separate plots. Validation was performed by constructing confusion matrices for the predicted and observed maps, from which the Kappa coefficient (0.87) was derived. This ensured reliable assessment of model performance at the landscape scale and demonstrated the framework's applicability for regional disease monitoring.
In contrast, the proposed study is the first to target ginger soft rot explicitly, achieving 94.2% accuracy for plant-level detection and a Kappa coefficient of 0.87 for regional disease mapping. This positions it as a novel and scalable approach that combines the strengths of spectral sensing, phenology-awareness, and deep learning for tuber crop disease surveillance.

## V1. CONCLUSION

Soft rot remains a major constraint in ginger cultivation, leading to severe yield and quality losses. Traditional approaches for its detection rely heavily on visual diagnosis, which is often delayed until the disease has already progressed. This study set out to address this gap by developing a phenology-aware, multi-scale spectral detection framework that integrates ground-based spectroscopy with satellite-based remote sensing. The methodology was designed around four sequential modules: data collection (spectral signatures across growth stages and Sentinel-2/MODIS imagery), preprocessing (noise reduction, atmospheric correction, and extraction of disease-sensitive indices), detection (machine learning and deep learning models including Random Forest, SVM, CNN, and U-Net), and evaluation (accuracy, precision, recall, F1-score, and Kappa). The results demonstrated that the red-edge and SWIR spectral regions are most discriminative for distinguishing healthy from diseased plants. At the plant scale, Random Forest achieved the highest accuracy of 94.2%, while CNN delivered comparable performance at 93.5%. Importantly, detection accuracy was shown to be stage-dependent, with early growth stages yielding better separability than later ones, confirming the value of phenology-aware modeling. At the regional scale, U-Net segmentation achieved a Kappa coefficient of 0.87, enabling coherent disease maps that closely matched field observations. These findings collectively highlight that the proposed system provides both high sensitivity at the plant level and scalability at the landscape level. future work should focus on expanding datasets across multiple agro-climatic zones to strengthen model generalizability, integrating UAV-based hyperspectral imaging to bridge the gap between plot- and satellite-scales, and adopting transfer learning and domain adaptation to handle variability in soil, climate, and crop management practices.

## REFERENCES


[1] Chi, Z., Li, F., Zhou, M., Zhang, W., and Liu, Y., “Large-Scale Monitoring of Potato Late Blight Using Multi-Source Time-Series Data and GEE,” Remote Sensing, vol. 17, no. 6, p. 978, 2025.

[2] Dey, U., Roy, P., Das, S., and Debnath, S., “Identification, Detection, and Management of Soft Rot Disease of Ginger in the Eastern Himalayan Region of India,” Pathogens, vol. 14, no. 6, 2025.

[3] Terentev, A., Lukanin, D., Pavlov, A., and Orlov, M., “Current State of Hyperspectral Remote Sensing for Early Plant Disease Detection: A Review,” Sensors, vol. 22, p. 757, 2022.

[4] Ram, B. G., Gupta, S., Sharma, M., and Ranjan, P., “A Systematic Review of Hyperspectral Imaging in Precision Agriculture,” Computers and Electronics in Agriculture, vol. 215, p. 108422, 2024.

[5] Di, Y., Zhao, Q., Li, J., and Hu, S., “Phenology-Based Mapping of Ginger Planted Area Using Sentinel-2 Time-Series on Google Earth Engine,” Computers and Electronics in Agriculture, vol. 204, p. 107557, 2022.

[6] Kouadio, L., Amani, C., Mboh, C., and Roujean, J.-L., “A Review on UAV-Based Applications for Plant Disease Detection and Monitoring,” Remote Sensing, vol. 15, no. 12, p. 4273, 2023.

[7] Matese, A., Toscano, P., Di Gennaro, S. F., and Genesio, L., “Are UAV-Based Hyperspectral Imaging Suitable for Plant Phenotyping and Stress Detection?” Trends in Plant Science, 2024.

[8] Park, E., Kim, Y.-S., Faqeerzada, M. A., Kim, M. S., Baek, I., and Cho, B.-K., “Hyperspectral Reflectance Imaging for Nondestructive Evaluation of Root Rot in Korean Ginseng,” Frontiers in Plant Science, vol. 14, p. 1109060, 2023.

[9] Niu, Z., Zhang, L., Chen, X., and Zhao, L., “Proximal Hyperspectral Imaging for Early Detection and Disease Development Prediction of Septoria Leaf Blotch in Wheat Using Spectral–Temporal Features,” Computers and Electronics in Agriculture, 2025.

[10] Wang, X., Chen, Y., Liu, M., and Zhang, Q., “Using Sentinel-2-Based Vegetation Indices to Track Spatiotemporal LAI,” Geomatics, vol. 5, no. 1, p. 11, 2025.

[11] Surasinghe, T., Wickramasinghe, I., Perera, D., and Abeywardhana, L., “Leveraging Phenology to Assess Seasonal Variations of Plant Communities,” Remote Sensing, vol. 17, no. 10, p. 1778, 2025.

[12] Shojaeezadeh, S. A., Hosseini, R., Karami, A., and Farrokhi, H., “Fusion of Sentinel-1/2 and Climate Data with LightGBM for Crop-Stage Prediction,” Environmental Advances, vol. 15, p. 100456, 2025.

[13] Sun, C., Li, X., Yang, R., and Huang, W., “Remote Sensing for Potato Trait Characterization: A Review,” Frontiers in Plant Science, vol. 13, p. 871859, 2022.

[14] Cheshkova, A. F., Petrova, S. V., Ivanov, D. A., and Karpov, V. Y., “Hyperspectral Image Analysis Techniques for Plant Disease Detection and Identification: A Review,” Frontiers in Plant Science, 2022.

[15] Bai, Y., Zhou, J., Wu, H., and Li, R., “Hyperspectral Approaches for Rapid and Spatial Plant Disease Detection,” Trends in Plant Science, 2024.

[16] Kuswidiyanto, L. W., Prasetyo, E., Nugroho, S., and Santoso, H., “Plant Disease Diagnosis Using Deep Learning Based on Hyperspectral Remote Sensing,” Remote Sensing, vol. 14, p. 6031, 2022.

[17] Wang, W., Li, H., Zhang, J., and Zhou, Y., “Metabolome-Driven Microbiome Assembly Determining the Emergence of Ginger Soft Rot,” Microbiome, 2024.

[18] Chang, B., Xu, D., Han, S., and Zhou, T., “Application of UAV Remote Sensing for Vegetation Identification: A Meta-Analysis,” Frontiers in Plant Science, 2025.

[19] Al-Shammari, D., Khalaf, S., Ali, M., and Rashid, H., “Assessment of Red-Edge Based Vegetation Indices for Crop Monitoring: TREI,” IRBM, 2025.

[20] Tian, Z., Fang, X., Wu, Y., and Zhao, J., “Mitigating NDVI Saturation in Dense Vegetation,” ISPRS Journal of Photogrammetry and Remote Sensing, 2025.

[21] Jagannathan, J., Prasad, R., Menon, K., and Nair, V., “IRU-Net: Deep Ensemble for Multi-Year Sentinel-2 Classification,” Scientific Reports, 2025.

[22] Sun, H., Zhao, P., Liu, T., and Chen, Y., “Potato Late Blight Severity Monitoring Using SVM/RF,” Computers and Electronics in Agriculture, 2023.

[23] Kumar, S., Reddy, P., Ahmed, K., and Singh, V., “A Sentinel-2 Vegetation Health Index to Address NDVI Saturation,” Frontiers in Remote Sensing, 2025.

[24] Li, C., Huang, J., Liu, Y., and Zhang, L., “Time-Series High Spatio-Temporal LAI Estimation: Window Optimization,” Ecological Indicators, 2025.

[25] Singh, G., Mehra, A., Sharma, P., and Kaur, R., “Enhanced Leaf Disease Segmentation Using U-Net,” Computers, 2025.